Engineering Strategy and Vector Library for the Rapid Generation of Modular Light-Controlled Protein–Protein Interactions

Alexandra-Madelaine Tichy[1,2,3], Elliot J. Gerrard[1,2,4], Julien M.D. Legrand[1,5], Robin M. Hobbs[1,5] and Harald Janovjak[1,2,3]

*1 - **Australian Regenerative Medicine Institute (ARMI),** Faculty of Medicine, Nursing and Health Sciences, Monash University, Clayton/Melbourne, VIC 3800, Australia*
*2 - **European Molecular Biology Laboratory Australia (EMBL Australia),** Monash University, Clayton/Melbourne, VIC 3800, Australia*
*3 - **Institute of Science and Technology Austria (IST Austria),** 3400 Klosterneuburg, Austria*
*4 - **Commonwealth Scientific and Industrial Research Organisation,** Synthetic Biology Future Science Platform, Monash University, Clayton/Melbourne, VIC 3800, Australia*
*5 - **Development and Stem Cells Program,** Monash Biomedicine Discovery Institute and Department of Anatomy and Developmental Biology, Monash University, Clayton/Melbourne, VIC 3800, Australia*

***Correspondence to Harald Janovjak:** Australian Regenerative Medicine Institute (ARMI), Faculty of Medicine, Nursing and Health Sciences, Monash University, 15 Innovation Walk, Clayton, VIC 3800, Australia. harald.janovjak@monash.edu*
https://doi.org/10.1016/j.jmb.2019.05.033

Abstract

Optogenetics enables the spatio-temporally precise control of cell and animal behavior. Many optogenetic tools are driven by light-controlled protein–protein interactions (PPIs) that are repurposed from natural light-sensitive domains (LSDs). Applying light-controlled PPIs to new target proteins is challenging because it is difficult to predict which of the many available LSDs, if any, will yield robust light regulation. As a consequence, fusion protein libraries need to be prepared and tested, but methods and platforms to facilitate this process are currently not available. Here, we developed a genetic engineering strategy and vector library for the rapid generation of light-controlled PPIs. The strategy permits fusing a target protein to multiple LSDs efficiently and in two orientations. The public and expandable library contains 29 vectors with blue, green or red light-responsive LSDs, many of which have been previously applied *ex vivo* and *in vivo*. We demonstrate the versatility of the approach and the necessity for sampling LSDs by generating light-activated caspase-9 (casp9) enzymes. Collectively, this work provides a new resource for optical regulation of a broad range of target proteins in cell and developmental biology.

Introduction

Optogenetics has revolutionized research in neuroscience, cell biology and developmental biology by allowing the "remote control" of cell and animal behavior with extraordinary precision [1–5]. This precision is achieved by utilizing light as a stimulus that offers unique advantages over pharmacological and genetic manipulation. For instance, light permits unparalleled control in time (e.g., to modulate animal behavior acutely or to target selected developmental or disease stages; Fig. 1A) and in space (e.g., to target selected compartments in a cell or selected cells in a tissue; Fig. 1B). Also, light can be readily applied and withdrawn given a sufficiently transparent matrix. Finally, light-activated molecular tools can be paired with genetic targeting to allow an even higher level of precision for specific cell types, tissues or developmental stages [6–10].

Optogenetics first flourished in the hands of neuroscientists that utilized animal and microbial opsins to dissect neural circuits through the bidirectional control of neuronal bioelectrical activity [8,11]. More recently and in cell types other than neurons, light control of gene regulation and cellular signaling, together with associated cell behaviors, has

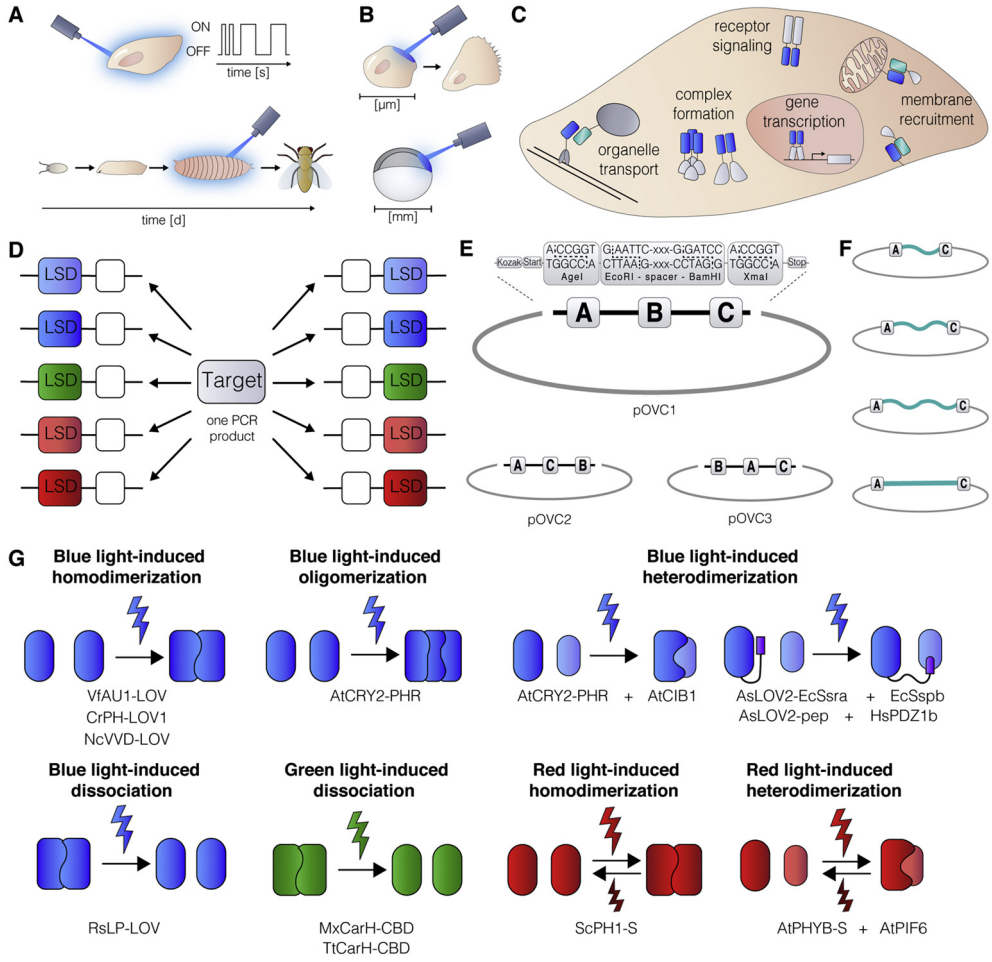

Fig. 1. Genetic engineering strategy and vector library for spatio-temporally precise regulation of cell and animal behavior. (A) The high temporal precision of light can be harnessed to study cellular responses to repetitive and complex inputs and to target specific developmental stages. (B) The high spatial precision of light can be harnessed to selectively activate processes in parts of cells or in specific tissues. (C) Optical control of many cellular processes relies on the regulation of PPIs by incorporating LSDs. (D) Engineering strategy based on a vector library that permits universal target amplicon insertion in a single cloning step (one digest, one ligation). (E) *ABC* and alternative cassettes to realize engineering strategy. Cassettes include Kozak sequence, start codon and stop codon. (F) *ABC* cassettes containing alternative linkers. (G) LSDs and their binding partners included in the library.

emerged [12,13]. The optogenetic tools that can regulate cell bioelectricity are fundamentally different from those applied to control biochemical and enzymatic processes. In the former case, ion-conducting opsins, such as channelrhodopsin or halorhodopsin, turn neurons on or off by changing their membrane potential through an intrinsic light-gated ion channel or pump activity [7,8,14]. In the latter case, a wide range of cellular processes have been rendered light-inducible by using light-sensitive domains (LSDs) that do not harbor catalytic activity but regulate intra- or intermolecular binding events (Fig. 1C).

LSDs are found in organisms from all domains of life and collectively respond not only to all visible but also to ultraviolet and far-red wavelengths [15–17]. Of particular importance in the field of optogenetics are light-oxygen-voltage sensing (LOV) domains and cryptochromes (CRYs) that bind flavins to sense blue light (maximal absorption wavelength ($\lambda_{max} \approx 450$ nm) [18–20] and phytochromes (PHYs) that utilize linear tetrapyrroles to sense red ($\lambda_{max} \approx 660$ nm) and far-red ($\lambda_{max} \approx 720$ nm) light [21–23]. In addition, green light-sensitive ($\lambda_{max} \approx 550$ nm) cobalamin binding domains (CBDs) that bind vitamin B_{12} derivatives were applied more recently [24,25]. The molecular consequences of photon absorption are either (i) light-induced unmasking of terminal peptides [26,27] for some LOV domains; (ii) light-induced homodimerization [18,19,21], homooligomerization [28] and heterodimerization with their respective accessory proteins

[20,22,29,30] for some LOV domains, CRYs and PHYs; or (iii) light-induced monomerization for some LOV domains, CBDs and UVR8 [24,31–33]. These functions have been harnessed in seminal studies to regulate the interactions and activity of diverse target proteins, such as small GTPases, kinases and transcription regulators [6,24,34–42].

The plethora of cellular processes governed by protein–protein interactions (PPIs) currently far exceeds the number of available optogenetic tools. This is in part because generating functional fusion proteins of LSDs and target proteins is a non-trivial task. For instance, multiple LSD genes need to be obtained and validated to find a suited domain, and the location of the fusion site as well as the length of linkers can be critical parameters that determine fusion protein function [43]. As a consequence of combinatorial complexity, many genetic constructs need to be generated and tested, and currently, no methods or libraries are available to facilitate this process.

Here, we developed a genetic engineering strategy and a vector library for the rapid and modular generation of light-controlled PPIs. The engineering strategy can produce LSD–target protein fusions in several domain orientations and with linkers in a single cloning step (a universal restriction enzyme digest followed by ligation) using inexpensive and readily available materials. The publicly available vector library contains a collection of prominent LSDs that are responsive to blue, green or red light and have been applied in the past *ex vivo* and *in vivo*. The design of the strategy and library allows for easy expansion either with further LSDs, targeting sequences or markers. Using this resource, we generated light-activated casp9 enzymes.

Results and Discussion

Efficient genetic engineering strategy

A major challenge in the optical control of PPIs is to achieve functional coupling of LSD oligomerization state changes to activity of target proteins. For most target proteins, it is initially unclear if a suited LSD can be identified and in what orientation LSDs are best attached because steric compatibility and effects on protein folding are difficult to predict. In the majority of previous studies, LSD–target protein fusions were constructed by inserting several LSD genes into vectors that contain the target protein (Sup. Fig. S1A, top). This approach requires selecting candidate LSDs, obtaining the corresponding genes from collaborators or commercial sources, validating LSD sequences, delineating domain boundaries and preparing amplicons that adapt each LSD to the target vector (Sup. Fig. S1A, bottom). Furthermore, generation of both N- and C-terminal fusion proteins may require additional modification of the vector and/or amplicons. We propose an inverted strategy in which the target protein is inserted into a series of vectors that already contain LSDs (Fig. 1D; see below for a comprehensive LSD vector library). The advantages of this strategy are that only a single amplicon of a familiar and available target gene is required and that multiple LSD–target protein fusions can be generated in a simple standardized reaction that is easily parallelized. As a consequence, multiple time-consuming steps that require analysis of sequences and reagents specific to each LSD are not required and the workflow is greatly simplified (Sup. Fig. S1B).

To achieve this strategy, we designed a modular cloning cassette termed *ABC* that harbors three insertion sites (*A*, *B* and *C*; Fig. 1E). Importantly, sites *A* and *C* contain recognition sequences for restriction enzymes that produce compatible cohesive overhangs (in both cases, a CCGG overhang after AgeI or XmaI digestion at site *A* and *C*, respectively; Fig. 1E). Consequently, a target protein amplicon flanked by either of these restriction sites in any combination can be inserted into site *A* as well as *C* and thus N- and C-terminally of a LSD (start and stop codons are already contained in the cassette). Site *B* contains recognition sequences for restriction enzymes of different families (EcoRI and BamHI) for incorporation of additional domains (e.g., fluorescent proteins) or epitopes. In order to provide additional flexibility, we engineered *ABC* vectors to include four different flexible or stiff linkers (Fig. 1F). We also prepared compatible *ACB* and *BAC* cassettes that permit insertion of flanking targeting sequences or fluorescent proteins in terminal *B* sites. Utilization of single and compatible restriction sites in site *A* and site *C* maximizes the likelihood that target proteins can be inserted without interference from internal restriction sites and minimizes required reagents. Furthermore, restriction enzymes are inexpensive and their application in the cassette retains advanced genetic engineering methods, such as those based on DNA recombination, for transfer of cassettes into other vectors. The promoter region in these vectors can be readily exchanged and promoters, and other regulatory sequences are generally part of species-specific or viral vectors. Overall, this genetic engineering strategy permits rapid generation of modular LSD–target protein fusions using readily available reagents.

LSD vector library

Employing above genetic engineering strategy, we generated 29 vectors that contain one of 11 LSDs or one of five LSD binding partners inserted into site *A* and *C* (Fig. 1G). These domains are the photolyase

homology region (PHR) domain of plant cryptochrome2 (AtCRY2-PHR of *Arabidopsis thaliana* [20,28]), LOV domains of plant, algal and fungal photoreceptors (two modified AsPT1-LOV2 domains of *Avena sativa*, CrPH-LOV1 of *Chlamydomonas reinhardtii* (the first LOV domain of the *Chlamydomonas* phototropin), NcVVD-LOV of *Neurospora crassa*, RsLP-LOV of *Rhodobacter sphaeroides* and VfAU1-LOV of *Vaucheria frigida* [18,19,26,29,30,32,44]), bacterial CBDs (MxCarH-CBD *of Myxococcus xanthus* and TtCarH-CBD of *Thermus thermophilus* [24]), and sensory modules of PHYs from cyanobacteria and plants (ScPH1-S of *Synechocystis PCC6803* and AtPHYB-S of *A. thaliana* [21,22,45]). The library also includes binding partners for the heterodimerizing LOV domains, CRY and PHY, which are the minimal proteins EcSspB of *E.coli* with different affinities, HsPDZ1b of *Homo sapiens*, AtCIB and AtPIF6 of *A. thaliana* [20,22,26,29,45] (Fig. 1G) (sequence information and protein database identifiers can be found in Table S1). Collectively, these vectors provide coverage of methods to induce homodimerization, homooligomerization, heterodimerization with binding partners, or monomerization in response to different wavelengths of light. Many of these domains have been previously utilized *ex vivo* and *in vivo* but the library also contains less frequently applied domains (e.g., the blue light-sensitive homodimerizing CrPH-LOV1 [44,46] or the monomerizing RsLP-LOV [32,33]). Vectors are available with all proteins inserted into the site *A* and separately the site *C* (i.e., N-terminal and C-terminal of the target protein insertion site), except in cases where attachment at one of the two termini is incompatible with robust protein function (AtPHYB functions most robustly when target proteins are attached to the C-terminus of this LSD, and AsPT1-LOV2 in the dimerizers when target proteins are fused of the N-terminus of this LSD). In the future, the library is expected to grow as its modular design allows direct expansion with additional LSDs [23,47].

Light-activated caspase-9

We employed the engineering strategy and vector library to develop a light-induced variant of caspase-9 (casp9), an initiator caspase in apoptosis induction. The function of casp9 is mediated by homomeric assembly through the N-terminal caspase recruitment domain (CARD) [48], and casp9 has been rendered inducible by substitution of CARD with orthogonal homodimerization domains [49,50]. This work demonstrated that dimerization by an N-terminal domain is sufficient for casp9 activation and resulted in a chemically-induced casp9 (iCasp9) that is employed as a cellular safety and suicide switch [51]. To generate casp9 activated by light (Opto-casp9), we inserted a casp9 amplicon N-terminally and C-terminally of three LOV domains and AtCRY2-PHR that undergo blue light-induced homodimerization or oligomerization (Fig. 2A). We focused on these LSDs because in general blue LSDs are commonly applied in optogenetics and because their flavin co-factors are ubiquitously available in cells of virtually all organisms. As a control, we employed casp9 fused to an engineered chemical dimerization domain derived from human FK506 binding protein (HsFKBP) analogous to iCasp9. We first tested if these proteins exhibit constitutive activity (i.e., dark activity) by metabolically assessing the viability of human embryonic kidney 293 (HEK293) cells using the fluorescent dye resazurin (Fig. 2B, C). As constitutive activity was not observed, we next tested if these proteins can be used to induce cell death. To analyze cell death while controlling for transfection efficiency, we co-transfected cells with Opto-casp9 and a genetic reporter (*Renilla* luciferase under the control of a constitutive promoter). We chose a luciferase over a fluorescent protein as the reporter gene because of the high signal-to-noise ratio in luminescence detection and to avoid undesired excitation of the reporter by stimulation light. Twenty-four hours after transfection, cells were stimulated for 7 h with blue light (continuous illumination, $\lambda \approx 470$ nm, intensity (I) = 200 μW/cm^2) in a tissue culture incubator equipped with light-emitting diodes, and luminescence signals were measured subsequently. We found strongly reduced luminescence signals for cells that were transfected with casp9 fused to VfAU1-LOV or AtCRY2-PHR domains but not the other domains (Fig. 2D, E). Interestingly, N-terminal but not C-terminal fusion of casp9 to CrPH-LOV1 resulted in increased luminescence signals, which may be explained by a dominant negative action of this LSD on basal levels of apoptosis or an alternative photoreaction mechanism. To confirm the specificity of the observed effect using VfAU1-LOV-casp9 as an example, we demonstrated that with increasing light-dose luminescence signals decrease (the half maximal effective light dose was 2.5 μW/cm^2; Sup. Fig. S2). We further verified that light stimulation resulted in apoptosis using flow cytometry analysis with propidium iodide (PI) and Annexin markers (Sup. Fig. S3A). For VfAU1-LOV-casp9 and AtCRY2-PHR-casp9 but not for mock transfected cells, we observed robust optical induction of apoptosis (Sup. Fig. S3B, C). This result demonstrates that by linking a casp9 amplicon to multiple LSDs and even without modification of the internal seven-residue linker functional Opto-casp9 enzymes could be quickly designed.

Specificity in light-induced PPIs

The modular genetic engineering strategy provides the possibility to perform additional

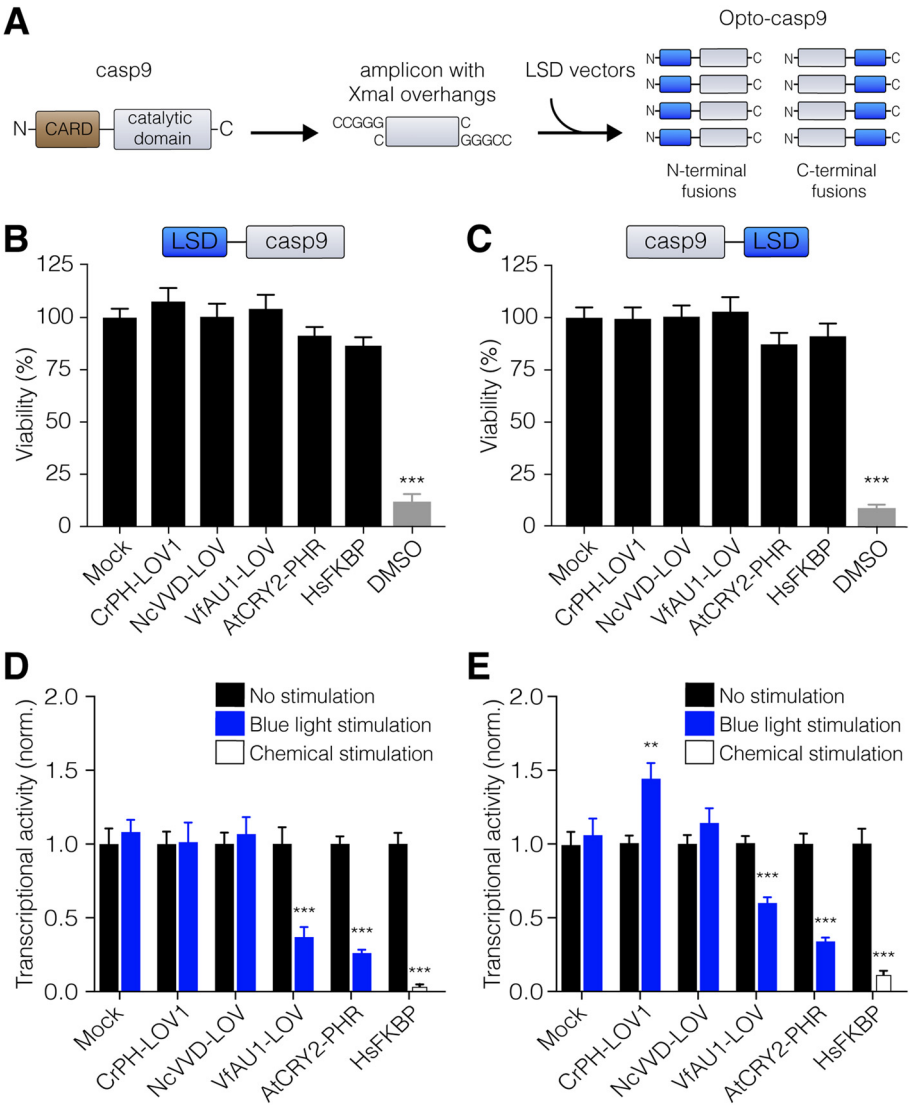

Fig. 2. Development of Opto-casp9 enzymes. (A) Procedure to engineer eight Opto-casp9 candidate enzymes starting from one casp9 catalytic domain amplicon and the vector library. (B and C) Viability of cultured human cells transfected with N- (B) and C-terminal (C) fusions of LSDs to casp9 assessed with resazurin. Twenty percent DMSO was employed as a positive control to induce cell death. (D and E) Light-induced reduction in transcriptional activity for cells transfected with N- (D) and C-terminal (E) fusions of LSDs to casp9 assessed using a luciferase reporter (7-h continuous blue light, $\lambda \approx 470$ nm, $I \approx 200$ µW/cm^2). For B–E: n = 12–20 (see Materials and Methods for details), four independent experiments, data shown are mean ± SEM. ** $p < 0.001$ or *** $p < 0.0001$. Two-tailed *t*-test.

experiments, such as negative controls and immunodetection, that complement the efficient fusion protein generation demonstrated above. In optogenetics, negative controls typically consist of the application of light to naïve cells or to cells that were transfected with inactivated optogenetic tools (e.g., through loss-of-function mutations). The latter control is required to obtain baseline signals and to ensure that overexpression of LSDs or target proteins does not alter cellular sensitivity. The most commonly applied loss-of-function mutations for inactivation either target photochemically active LSD residues or residues involved in light-induced conformational changes. However, targeting LSD photochemistry can be incomplete with persistent LSD activation through alternative reaction mechanisms or generation of chemical photoreaction side products [52,53]. In addition, because of the diversity in the structures and activation mechanisms of LSDs, generalizable loss-of-function mutations do not exist, and thus, negative controls cannot be studied under identical conditions. To address these limitations, we developed a universal inactivation strategy for light-controlled PPIs, which is based on

testing constructs in which the LSD and target protein have been uncoupled (e.g., uncoupling of VfAU1-LOV and casp9 should result in lost light activation). We realized this strategy by taking advantage of the availability of site *B* in all generated vectors and the opportunity of designing linkers with additional functionality. Into this site, we inserted a self-cleaving peptide sequence of porcine teschovirus-1 2A (P2A) that will effectively dissociate the two domains resulting in a loss of light sensitivity (Fig. 3A). As expected for a P2A-modified Opto-casp9, we observed that self-cleavage completely abolished light-induced changes in the luminescence signals, effectively producing the same outcome as removal of the catalytic activity of casp9 (Fig. 3B, Sup. Fig. S4). Immunoblotting against epitope tags that flanked the P2A sequence verified cleavage as we only detected the single LSD and casp9 domains but not the full protein (Fig. 3C). These results demonstrate a new control strategy that preserves target protein and LSD expression and LSD photochemistry taking advantage of linker and epitope incorporation into site *B*.

Conclusions

Optogenetics is one of few techniques that permit the regulation of cell behaviors with high precision in space and time. We developed a resource for the generation of light-induced PPIs and demonstrated its applicability by engineering Opto-casp9 enzymes. This resource will contribute to the broader use of optogenetics in cell and developmental biology and pave the way to novel optogenetics studies. For instance, experiments on the scale of entire families of LSDs or of target proteins require efficient and modular genetic engineering approaches that are now within reach. These experiments could also test if a forced PPI is sufficient for (in)activation of a protein, conceptually similar to a recent study in which light induced the signaling of orphan receptors [54]. Opto-casp9 enzymes may provide a test bed for optogenetic hardware development and testing, a process that entails optimization of light parameters (e.g., wavelength, intensity, duration) and culture conditions, because cell death can be assessed with different assays. Finally, the

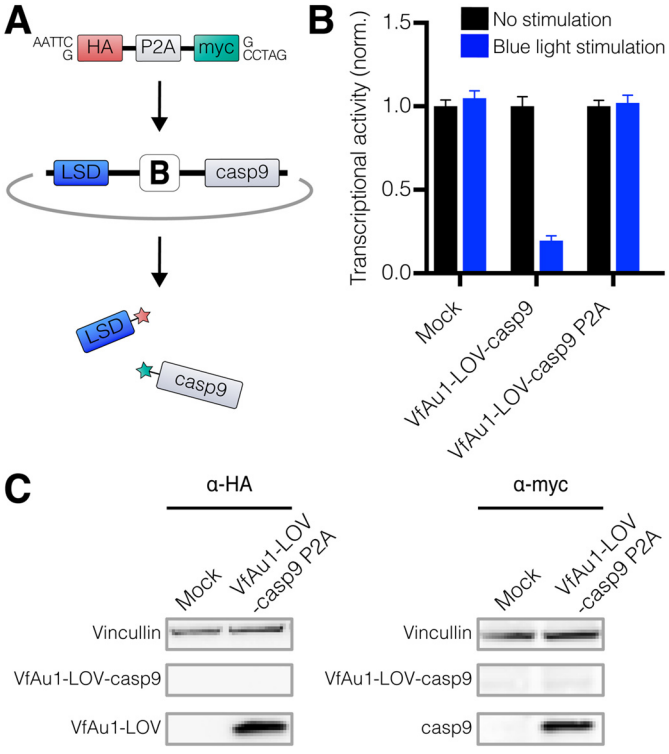

Fig. 3. Control experiments with self-cleaving epitope-linker. (A) Incorporation of a P2A sequence results in self-cleavage and separation of LSD and target protein. (B) Light-induced cell death for cells transfected with vectors containing the self-cleaving linker (7-h continuous blue light, $\lambda \approx 470$ nm, $I \approx 200$ μW/cm^2). (C) Immunoblotting to validate efficient cleavage. For B: n = 12, four independent experiments, data shown are mean ± SEM. *** $p < 0.0001$. Two-tailed *t*-test.

engineering strategy and empty cassettes may also be of use in areas other than optogenetics, such as for the rapid and modular design of fluorescent sensors and protein probes.

Materials and Methods

Cassette design

Cassettes were introduced in pcDNA3.1- (Invitrogen/Life Technologies) to generate the vectors named pOVC1–3 (optogenetic vector core 1–3, Sup. Fig. S5). A XmaI restriction site was removed from the backbone using site-directed mutagenesis (oligonucleotides 1 and 2, Table S2). Inverse polymerase chain reactions (PCR) (oligonucleotides 3 and 4, 5 and 6, and 7 and 8) were applied to remove the vector multiple cloning site and create *ABC* (pOVC1), *ACB* (pOVC2) and *BAC* (pOVC3) cassettes. In the inverse PCR procedure, PCR products were digested with DpnI, digested with EcoRI, XmaI or AgeI (NEB), respectively, ligated for 3 h at room temperature (RT) or overnight at 4 °C using T4 ligase (Promega), and propagated in *Escherichia coli* XL10 Gold cells (Agilent). All cassettes contain Kozak sequences, start codons and stop codons [for backbone ABC, the stop codon was introduced using site-directed mutagenesis in a separate reaction (oligonucleotides 9 and 10)]. For linker insertion, backbone pOVC1 was digested using EcoRI and BamHI. Linker fragments were generated by inverse PCR (oligonucleotides 57 and 58) or by annealing and phosphorylating single stranded oligonucleotides (59 to 64). All vector sequences (Table S3) were verified by Sanger sequencing (Micromon, Monash University) and deposited at Addgene.org.

LSD amplification and vector library

LSDs were amplified using PCR and oligonucleotides with AgeI and/or XmaI restriction site overhangs (oligonucleotides 11 to 34 and 45 to 52). Templates were previously described vectors from our laboratory or obtained from Addgene.org (Table S1). In addition, gene fragments of AtCRY2-PHR, ScPH-1, AsLOV2-EcSsra, EcSSPB micro, AsLOV2-pep and HsPDZ1b were synthesized by a commercial supplier (Integrated DNA Technologies; Table S4). Restriction sites for AgeI and BamHI were removed from ScPH1-S and AtPHYB-S, respectively, as well as XmaI restriction sites from HsFKBP and AtCRY2-PHR using site-directed mutagenesis (oligonucleotides 35 to 42). Site-directed mutagenesis was used to create EcSSPB nano (oligonucleotides 65 and 66). PCR products were digested with DpnI and with AgeI, XmaI or AgeI and XmaI depending on oligonucleotide overhangs. Backbone pOVC1 was digested with AgeI or XmaI for insertion into site *A* or *C*, respectively, and phosphatase treated. Backbone and inserts were ligated either for 3 h at RT or overnight at 4 °C using T4 ligase (Promega). All vector sequences (Table S5) were verified by Sanger sequencing (LGC Genomics) and deposited at Addgene.org. Note that for future subcloning of the generated genes, universal oligonucleotides can be designed that contain recognition sites for the enzymes AflII, ApaI, AscI, FseI, PacI, PspOMI or SbfI as these are not found in any of the genes.

Opto-casp9 constructs

The catalytic domain of casp9 (residues 135–416 of UniProt entry P55211) was synthesized (Integrated DNA Technologies; Table S4), amplified by PCR (oligonucleotides 43 and 44) and digested with XmaI. Vectors were digested with XmaI or AgeI, respectively, treated with phosphatase and gel purified. Backbone vectors and casp9 insert were ligated either for 3 h at RT or overnight at 4 °C using T4 ligase. Site-directed mutagenesis was used to introduce point substitution C287A into the catalytic domain of casp9 in VfAU1-LOV-casp9 and HsFKBP-casp9 (oligonucleotides 55 and 56). HA-P2A-myc was synthesized as a gene fragment (Integrated DNA Technologies, Table S4), amplified using PCR and restriction site overhangs (oligonucleotides 53 and 54), and inserted into site *B* of VfAU1-LOV-casp9 using EcoRI and BamHI. All vector sequences (Table S6) were verified by Sanger sequencing (Micromon, Monash University) and deposited at Addgene.org.

Cell culture and transfection

HEK293 cells (Thermo Fisher Scientific; further authenticated by assessing cell morphology and growth rate) were cultured in mycoplasma-free Dulbecco's modified eagle medium (Thermo Fisher Scientific) in a humidified incubator with 5% CO_2 atmosphere at 37 °C. Medium was supplemented with 10% FBS, 100 U/ml penicillin and 0.1 mg/ml streptomycin (Thermo Fisher Scientific). On the day after seeding, cells were transfected in Dulbecco's modified eagle medium supplemented with 5% FBS using polyethylenimine (Polysciences). Media was changed after 4 to 6 h, and cells were stimulated with light starting 24 h after transfection for the durations specified below and at the intensities specified in the main text.

Light stimulation of cells

For light stimulation of cells, a tissue culture incubator was equipped with 150 light-emitting

diodes (SMD5050-RGB on a LED strip at 3.3-cm spacing). Light intensity was adjusted with a dimmer and measured with a digital power meter (LP1, Sanwa). To obtain light dose curve (Sup. Fig. S2), one to four layers of neutral density filters (Filter 210, LEE Filters) were used to reduce intensity of selected wells.

Metabolic and transcriptional assays

HEK293 cells (2.5×10^4) were seeded in each well of white bottom 96-well plates (Costar) and maintained as described above. Cells were transfected with 200 ng vector (casp9, renilla luciferase reporter and empty vector at a ratio of 10:1:9) as described above. Twenty-four hours after transfection, cells were either stimulated with blue light ($\lambda \approx 470$ nm), 10 nM of the chemical dimerizer AP20187 (ClonTech Laboratories) or left unstimulated. Light and AP20187 were applied for 7 h continuously. Unstimulated cells were kept in the dark for 6 h before addition of resazurin (Sigma) at a final concentration of 55 µM. After incubation for 1 h, resazurin fluorescence was measured in a plate reader (excitation 540 ± 15 nm, emission 590 ± 20 nm, ClarioSTAR, BMGLabtech). Viability was defined as relative fluorescence units compared to a mock-transfected control. Immediately after resazurin assays, stimulated and unstimulated cells were washed once with phosphate-buffered saline (PBS), lysed and processed with homemade luciferase reporter reagents [24]. Luminescence was measured in the plate reader and transcriptional activity was defined as mean raw luminescence values.

Flow cytometry

HEK293 cells (5×10^5) in each well of clear 6-well plates (Costar) were transfected with 2 µg vector (casp9 and empty vector at a ratio of 1:1) as described above. Twenty-four hours after transfection, cells were either stimulated with light (continuous blue light, $\lambda \approx 470$ nm, $I \approx 200$ µW/cm^2) or protected from light for 7 h at 37 °C. After incubation, cells were collected, washed once with ice-cold PBS (Thermo Fisher Scientific) supplemented with 2% FBS and stained with FITC-AnnexinV/PI Apoptosis Detection Kit according to manufacturer's instructions (BioLegend). Samples were then run on a LSRFortessa X-20 flow cytometer (BD Biosciences), and data were analyzed with FlowJo software (FlowJo).

Immunoblotting

HEK293 cells (5×10^5) in each well of clear 6-well plates (Costar) were transfected with 2 µg vector as described above. Twenty-four hours after transfection, cells were washed once with ice-cold PBS and lysed on ice in 180 µl lysis buffer [150 mM NaCl, 1% TritonX-100, 0.1% SDS, 0.5% sodium deoxycholate, 50 mM Tris, complete protease inhibitor (Roche)]. Lysates were shaken for 30 min at 4 °C and centrifuged for 20 min at 12,000*g*. Lysate (30 µl) per lane was separated by SDS-PAGE and electroblotted onto PVDF membranes. Blots were incubated with primary antibodies (HA-Tag no. 2367, dilution 1:1000; myc-Tag no. 2276, dilution 1:1000; Cell Signaling Technology; Vincullin ab129002, dilution 1:10000; Abcam) in blocking solution (5% BSA in TBS-T) overnight at 4 °C. Secondary antibody (goat anti-rabbit IgG(H + L)-HRP conjugate, goat anti-mouse IgG(H + L)-HRP, dilution 1:10000, Biorad) was applied for 1 h at RT, and blots were developed with Carity™ Western ECL Substrate (Biorad).

Statistical analysis

Results were evaluated using Prism (GraphPad). Differences between stimulated and unstimulated samples were analyzed using two-tailed *t*-tests, and *p* values are given in the figure captions. Sample numbers (n) and the number of independent experiments (biological replicates) for each bar are specified in the figure captions, except for Fig. 2B–E. In Fig. 2B, sample numbers are 14, except for mock (26), HsFKBP (15) and DMSO (13). In Fig. 2C, sample numbers are 16, except for mock (25), HsFKBP (19) and DMSO (12). In Fig. 2D, sample numbers are 14, except for HsFKBP (26 and 12, dark and light). In Fig. 2E, sample numbers are 16, except for mock (28) and HsFKBP (28 and 12, dark and light) and DMSO (12).

CRediT authorship contribution statement

Alexandra-Madelaine Tichy: Conceptualization, Data curation, Formal analysis, Investigation, Methodology, Validation, Visualization, Writing - original draft, Writing - review & editing. **Elliot J. Gerrard:** Data curation, Formal analysis, Investigation, Methodology, Validation, Visualization, Writing - review & editing. **Julien M.D. Legrand:** Data curation, Formal analysis, Methodology, Resources, Validation, Visualization, Writing - review & editing. **Robin M. Hobbs:** Formal analysis, Funding acquisition, Methodology, Resources, Validation, Writing - review & editing. **Harald Janovjak:** Conceptualization, Data curation, Formal analysis, Funding acquisition, Methodology, Project administration, Resources, Supervision, Validation, Visualization, Writing - original draft, Writing - review & editing.

Acknowledgments

We thank M. De Seram for assistance with experiments; E. Gschaider-Reichhart and S. Kainrath for discussions; and C. Tucker and C. Voigt for LSD genes. We acknowledge the facilities, scientific and technical assistance of Micromon and FlowCore at Monash University. The Australian Regenerative Medicine Institute is supported by grants from the State Government of Victoria and the Australian Government. The EMBL Australia Partnership Laboratory (EMBL Australia) is supported by the National Collaborative Research Infrastructure Strategy of the Australian Government. Elliot J. Gerrard was funded through the CSIRO Synthetic Biology Future Science Platform.

Competing Interests: The authors report no conflict of interest.

Preprint: http://www.biorxiv.org/content/10.1101/583369v1.

Appendix A. Supplementary data

Supplementary data to this article can be found online at https://doi.org/10.1016/j.jmb.2019.05.033.

Received 30 March 2019;
Received in revised form 20 May 2019;
Available online 29 May 2019

KeywordsOptogenetics;
light-sensitive domain;
photoreceptor;
protein-protein interaction;
caspase9

Abbreviations used:
LSD, light-sensitive domain; LOV, light-oxygen-voltage sensing; CRY, cryptochrome; PHY, phytochrome; CBD, cobalamin binding domain; PPI, protein–protein interaction; PHR, photolyase homology region; P2A, porcine teschovirus-1 2A; PCR, polymerase chain reaction; RT, room temperature; casp9, caspase-9.

References

[1] E. Pastrana, Optogenetics: controlling cell function with light, Nat. Methods 8 (2011) 24–25.
[2] A. Reiner, E.Y. Isacoff, The brain prize 2013: the optogenetics revolution, Trends Neurosci. 36 (2013) 557–560.
[3] K.M. Tye, K. Deisseroth, Optogenetic investigation of neural circuits underlying brain disease in animal models, Nat. Rev. Neurosci. 13 (2012) 251–266.
[4] S.C. Williams, K. Deisseroth, Optogenetics, Proc. Natl. Acad. Sci. U. S. A. 110 (2013) 16287.
[5] K.E. Brechun, K.M. Arndt, G.A. Woolley, Strategies for the photo-control of endogenous protein activity, Curr. Opin. Struct. Biol. 45 (2017) 53–58.
[6] H.E. Johnson, Y. Goyal, N.L. Pannucci, T. Schupbach, S.Y. Shvartsman, J.E. Toettcher, The spatiotemporal limits of developmental Erk signaling, Dev. Cell 40 (2017) 185–192.
[7] F. Zhang, L.P. Wang, M. Brauner, J.F. Liewald, K. Kay, N. Watzke, et al., Multimodal fast optical interrogation of neural circuitry, Nature. 446 (2007) 633–639.
[8] E.S. Boyden, F. Zhang, E. Bamberg, G. Nagel, K. Deisseroth, Millisecond-timescale, genetically targeted optical control of neural activity, Nat. Neurosci. 8 (2005) 1263–1268.
[9] L. Kowalik, J.K. Chen, Illuminating developmental biology through photochemistry, Nat. Chem. Biol. 13 (2017) 587–598.
[10] G. Guglielmi, H.J. Falk, S. De Renzis, Optogenetic control of protein function: from intracellular processes to tissue morphogenesis, Trends Cell Biol. 26 (2016) 864–874.
[11] B.V. Zemelman, G.A. Lee, M. Ng, G. Miesenbock, Selective photostimulation of genetically chARGed neurons, Neuron. 33 (2002) 15–22.
[12] J.E. Toettcher, O.D. Weiner, W.A. Lim, Using optogenetics to interrogate the dynamic control of signal transmission by the Ras/Erk module, Cell. 155 (2013) 1422–1434.
[13] K. Muller, W. Weber, Optogenetic tools for mammalian systems, Mol. BioSyst. 9 (2013) 596–608.
[14] G. Nagel, T. Szellas, W. Huhn, S. Kateriya, N. Adeishvili, P. Berthold, et al., Channelrhodopsin-2, a directly light-gated cation-selective membrane channel, Proc. Natl. Acad. Sci. U. S. A. 100 (2003) 13940–13945.
[15] A. Moglich, X. Yang, R.A. Ayers, K. Moffat, Structure and function of plant photoreceptors, Annu. Rev. Plant Biol. 61 (2010) 21–47.
[16] M. Heijde, R. Ulm, UV-B photoreceptor-mediated signalling in plants, Trends Plant Sci. 17 (2012) 230–237.
[17] J.M. Ortiz-Guerrero, M.C. Polanco, F.J. Murillo, S. Padmanabhan, M. Elias-Arnanz, Light-dependent gene regulation by a coenzyme B12-based photoreceptor, Proc. Natl. Acad. Sci. U. S. A. 108 (2011) 7565–7570.
[18] M. Grusch, K. Schelch, R. Riedler, E. Reichhart, C. Differ, W. Berger, et al., Spatio-temporally precise activation of engineered receptor tyrosine kinases by light, EMBO J. 33 (2014) 1713–1726.
[19] X. Wang, X. Chen, Y. Yang, Spatiotemporal control of gene expression by a light-switchable transgene system, Nat. Methods 9 (2012) 266–269.
[20] M.J. Kennedy, R.M. Hughes, L.A. Peteya, J.W. Schwartz, M. D. Ehlers, C.L. Tucker, Rapid blue-light-mediated induction of protein interactions in living cells, Nat. Methods 7 (2010) 973–975.
[21] E. Reichhart, A. Ingles-Prieto, A.M. Tichy, C. McKenzie, H. Janovjak, A phytochrome sensory domain permits receptor activation by red light, Angew. Chem. Int. Ed. Engl. 55 (2016) 6339–6342.
[22] A. Levskaya, O.D. Weiner, W.A. Lim, C.A. Voigt, Spatiotemporal control of cell signalling using a light-switchable protein interaction, Nature. 461 (2009) 997–1001.
[23] T.A. Redchuk, E.S. Omelina, K.G. Chernov, V.V. Verkhusha, Near-infrared optogenetic pair for protein regulation and spectral multiplexing, Nat. Chem. Biol. 13 (2017) 633–639.
[24] S. Kainrath, M. Stadler, E. Reichhart, M. Distel, H. Janovjak, Green-light-induced inactivation of receptor signaling using cobalamin-binding domains, Angew. Chem. Int. Ed. Engl. 56 (2017) 4608–4611.
[25] M. Jost, J. Fernandez-Zapata, M.C. Polanco, J.M. Ortiz-Guerrero, P.Y. Chen, G. Kang, et al., Structural basis for

gene regulation by a B12-dependent photoreceptor, Nature. 526 (2015) 536–541.
[26] O.I. Lungu, R.A. Hallett, E.J. Choi, M.J. Aiken, K.M. Hahn, B. Kuhlman, Designing photoswitchable peptides using the AsLOV2 domain, Chem. Biol. 19 (2012) 507–517.
[27] Y.I. Wu, D. Frey, O.I. Lungu, A. Jaehrig, I. Schlichting, B. Kuhlman, et al., A genetically encoded photoactivatable Rac controls the motility of living cells, Nature. 461 (2009) 104–108.
[28] L.J. Bugaj, A.T. Choksi, C.K. Mesuda, R.S. Kane, D.V. Schaffer, Optogenetic protein clustering and signaling activation in mammalian cells, Nat. Methods 10 (2013) 249–252.
[29] G. Guntas, R.A. Hallett, S.P. Zimmerman, T. Williams, H. Yumerefendi, J.E. Bear, et al., Engineering an improved light-induced dimer (iLID) for controlling the localization and activity of signaling proteins, Proc. Natl. Acad. Sci. U. S. A. 112 (2015) 112–117.
[30] D. Strickland, Y. Lin, E. Wagner, C.M. Hope, J. Zayner, C. Antoniou, et al., TULIPs: tunable, light-controlled interacting protein tags for cell biology, Nat. Methods 9 (2012) 379–384.
[31] D. Chen, E.S. Gibson, M.J. Kennedy, A light-triggered protein secretion system, J. Cell Biol. 201 (2013) 631–640.
[32] K.S. Conrad, A.M. Bilwes, B.R. Crane, Light-induced subunit dissociation by a light-oxygen-voltage domain photoreceptor from *Rhodobacter sphaeroides*, Biochemistry. 52 (2013) 378–391.
[33] F. Richter, I. Fonfara, B. Bouazza, C.H. Schumacher, M. Bratovic, E. Charpentier, et al., Engineering of temperature- and light-switchable Cas9 variants, Nucleic Acids Res. 44 (2016) 10003–10014.
[34] E. Izquierdo, T. Quinkler, S. De Renzis, Guided morphogenesis through optogenetic activation of Rho signalling during early *Drosophila* embryogenesis, Nat. Commun. 9 (2018) 2366.
[35] X. Wang, L. He, Y.I. Wu, K.M. Hahn, D.J. Montell, Light-mediated activation reveals a key role for Rac in collective guidance of cell movement in vivo, Nat. Cell Biol. 12 (2010) 591–597.
[36] S.K. Yoo, Q. Deng, P.J. Cavnar, Y.I. Wu, K.M. Hahn, A. Huttenlocher, Differential regulation of protrusion and polarity by PI3K during neutrophil motility in live zebrafish, Dev. Cell 18 (2010) 226–236.
[37] V.V. Krishnamurthy, J.S. Khamo, W. Mei, A.J. Turgeon, H.M. Ashraf, P. Mondal, et al., Reversible optogenetic control of kinase activity during differentiation and embryonic development, Development. 143 (2016) 4085–4094.
[38] K. Sako, S.J. Pradhan, V. Barone, A. Ingles-Prieto, P. Muller, V. Ruprecht, et al., Optogenetic control of nodal signaling reveals a temporal pattern of nodal signaling regulating cell fate specification during gastrulation, Cell Rep. 16 (2016) 866–877.
[39] A. Reade, L.B. Motta-Mena, K.H. Gardner, D.Y. Stainier, O. D. Weiner, S. Woo, TAEL: a zebrafish-optimized optogenetic gene expression system with fine spatial and temporal control, Development. 144 (2017) 345–355.
[40] H.M. Beyer, S. Juillot, K. Herbst, S.L. Samodelov, K. Muller, W.W. Schamel, et al., Red light-regulated reversible nuclear localization of proteins in mammalian cells and zebrafish, ACS Synth. Biol. 4 (2015) 951–958.
[41] P. Vopalensky, S. Pralow, N.L. Vastenhouw, Reduced expression of the nodal co-receptor Oep causes loss of mesendodermal competence in zebrafish, Development. 145 (2018).
[42] V. Barone, M. Lang, S.F.G. Krens, S.J. Pradhan, S. Shamipour, K. Sako, et al., An effective feedback loop between cell–cell contact duration and morphogen signaling determines cell fate, Dev. Cell 43 (2017) 198–211 e112.
[43] F. Kawano, R. Okazaki, M. Yazawa, M. Sato, A photo-activatable Cre-loxP recombination system for optogenetic genome engineering, Nat. Chem. Biol. 12 (2016) 1059–1064.
[44] R.J. Kutta, E.S. Hofinger, H. Preuss, G. Bernhardt, B. Dick, Blue-light induced interaction of LOV domains from *Chlamydomonas reinhardtii*, Chembiochem. 9 (2008) 1931–1938.
[45] S. Shimizu-Sato, E. Huq, J.M. Tepperman, P.H. Quail, A light-switchable gene promoter system, Nat. Biotechnol. 20 (2002) 1041–1044.
[46] Y. Nakasone, M. Ohshima, K. Okajima, S. Tokutomi, M. Terazima, Photoreaction dynamics of LOV1 and LOV2 of phototropin from *Chlamydomonas reinhardtii*, J. Phys. Chem. B 122 (2018) 1801–1815.
[47] X.X. Zhou, H.K. Chung, A.J. Lam, M.Z. Lin, Optical control of protein activity by fluorescent protein domains, Science. 338 (2012) 810–814.
[48] M. Renatus, H.R. Stennicke, F.L. Scott, R.C. Liddington, G.S. Salvesen, Dimer formation drives the activation of the cell death protease caspase 9, Proc. Natl. Acad. Sci. U. S. A. 98 (2001) 14250–14255.
[49] Y. Nihongaki, H. Suzuki, F. Kawano, M. Sato, Genetically engineered photoinducible homodimerization system with improved dimer-forming efficiency, ACS Chem. Biol. 9 (2014) 617–621.
[50] K.C. Straathof, M.A. Pule, P. Yotnda, G. Dotti, E.F. Vanin, M. K. Brenner, et al., An inducible caspase 9 safety switch for T-cell therapy, Blood. 105 (2005) 4247–4254.
[51] A. Di Stasi, S.K. Tey, G. Dotti, Y. Fujita, A. Kennedy-Nasser, C. Martinez, et al., Inducible apoptosis as a safety switch for adoptive cell therapy, N. Engl. J. Med. 365 (2011) 1673–1683.
[52] E.F. Yee, R.P. Diensthuber, A.T. Vaidya, P.P. Borbat, C. Engelhard, J.H. Freed, et al., Signal transduction in light-oxygen-voltage receptors lacking the adduct-forming cysteine residue, Nat. Commun. 6 (2015), 10079.
[53] X. Shu, V. Lev-Ram, T.J. Deerinck, Y. Qi, E.B. Ramko, M.W. Davidson, et al., A genetically encoded tag for correlated light and electron microscopy of intact cells, tissues, and organisms, PLoS Biol. 9 (2011), e1001041.
[54] M. Morri, I. Sanchez-Romero, A.M. Tichy, S. Kainrath, E.J. Gerrard, P.P. Hirschfeld, et al., Optical functionalization of human class A orphan G-protein-coupled receptors, Nat. Commun. 9 (2018) 1950.